CHEMICAL ENGINEERING TRANSACTIONS
VOL. 45, 2015
A publication of AIDIC
The Italian Association of Chemical Engineering
www.aidic.it/cet
Guest Editors: Petar Sabev Varbanov, Jiří Jaromír Klemeš, Sharifah Rafidah Wan Alwi, Jun Yow Yong, Xia Liu
Copyright © 2015, AIDIC Servizi S.r.l.,
ISBN 978-88-95608-36-5; **ISSN** 2283-9216
DOI: 10.3303/CET1545033

Combustion Performance of a Counter-Rotating Double Swirl Flame Burner under Stratified Burning Condition

Cheng Tung Chong*[a], Shu Shiung Lam[b], Simone Hochgreb[c]

[a]Faculty of Mechanical Engineering, Universiti Teknologi Malaysia 81310 Skudai, Johor, Malaysia.
[b]Eastern Corridor Renewable Energy Group (ECRE), School of Ocean Engineering, University Malaysia Terengganu, 21030 Kuala Terengganu, Terengganu, Malaysia.
[c]Department of Engineering, University of Cambridge, Trumpington Street, CB2 1PZ Cambridge, UK.
ctchong@mail.fkm.utm.my

A double-annulus counter-rotating premixed swirl burner was utilised to investigate the effect of varied air flow and equivalence ratio between the inner and outer annulus on the flame structure and emission performance. The air and methane gaseous fuel for each annulus were independently premixed at the plenum prior to combustion at atmospheric condition. Imaging of OH* chemiluminescence was performed to obtain the flame structure of stratified flames. Higher swirl flow for richer mixture in the inner annulus generates an elongated and enlarged area of flame reaction zone due to increased flame intensity. Emission measurements show the arrangement of leaner inner/outer richer premixed air/fuel produce emissions comparable to baseline case of homogenous mixture and flow. Under the arrangement of stratified mixture of richer inner/leaner outer annulus, significant higher emissions of CO, NO and NO_2 were shown. Variation of the air flow split ratio between the annuluses affects emissions, in particular, higher inner/lower outer swirl flow arrangement results in higher emission rates under rich inner/lean outer mixture stratification.

1. Introduction

Swirl flame is utilised in many practical combustion devices including gas turbines, furnaces, boilers and internal combustion engines. The wide use of swirl flame in practical system is due to the virtue of compact, short and intense turbulent flame that offers good flame stability. To date, study of swirl flames have mainly concentrated on single swirl burner. Detailed characterisation of flow field, interaction of flame with droplets in combustor have been extensively performed and documented (Beer and Chigier, 1972). A single swirl axial burner was utilised to investigate the spray (Chong and Hochgreb, 2015) and combustion characteristics of biodiesel (Chong and Hochgreb, 2014). Vondál and Hájek (2012) investigated the swirl flow pattern of a model swirl combustor numerically and compared with experimental data. Sorrentino et al. (2015) designed a burner for flameless combustion using swirl flow. The benefit of swirl flow in combustor includes the creation of large recirculation flow that assists in flame stabilization (Chong and Hochgreb, 2015). Although interest in using double annulus swirl burner for combustion has been proposed, characterisation and performance evaluation of these burner are relatively scarce.

Gupta et al. (1998) reported that double annulus swirl flame burner presents the advantage of enabled control of radial distribution of flow and the degree of swirl to achieve stable flames over a wide range of operating conditions. The flame characteristics however, differ significantly from single swirl flame. Merkle et al. (2003) examined the turbulent flow and mixture field of an airblast spray enveloped by two annuluses of co-swirling and counter-swirling streams of air flow. The counter-swirl arrangement was reported to exhibit increased strength of internal recirculation zone with shorter axial length, but lesser turbulent exchange of momentum perpendicular to the main flow compared to the co-swirl configuration. Another study reported that counter-swirl airblast spray configuration increases the radial dispersion of flow and promotes mixing. Further, the flame stability limits was reported to have improved with lower lean blow off limit due to increased strength of recirculation zone that assists in the transport of fuel droplets (Ateshkadi

Please cite this article as: Chong C.T., Lam S.S., Hochgreb S., 2015, Combustion performance of a counter-rotating double swirl flame burner under stratified burning condition, Chemical Engineering Transactions, 45, 193-198 DOI:10.3303/CET1545033

et al., 1998). Emissions of NO_x of a double swirl combustor was lower compared to a single swirl, non-premixed, direct central fuel injection burner (Terasaki and Hayashi, 1996). The double annulus co-rotating swirl burner was reported to emit the lowest quantity of NO_x under lean condition. The improved emission characteristic was attributed to the rapid mixing process that generates uniform equivalence ratio profile in the combustion region.

Due to the lack of data on counter-rotating swirl flames, the present experiment examines the flame structure of counter-rotating stratified flames with varied air flow between the two annuluses. Flame imaging technique was utilised to map the global flame reaction zone and to derive the planar flame structure. The emission performance of double swirl flame relative to baseline case is investigated.

2. Experimental

2.1 Burner setup and flow delivery system

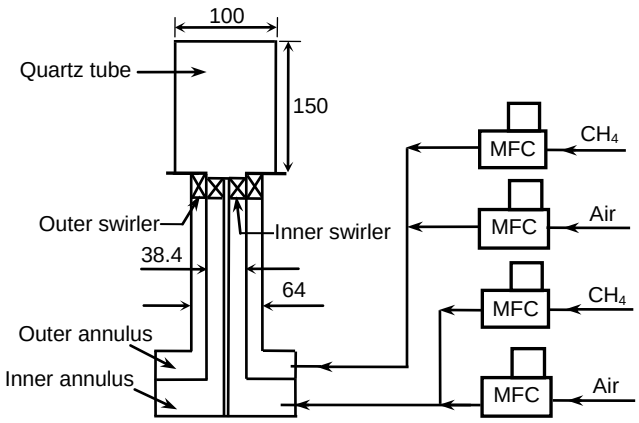

Figure 1: Schematic of the counter-swirl burner and flow delivery system. Dimensions are in mm

The present swirl flame burner consists of two annuluses with two swirlers placed at the burner outlet. The internal swirler in the inner annulus has eight straight vanes fixed at the angle of 45^o from the centreline axial axis. The outer swirler comprises of ten straight vanes attached to the swirler hub at the angle of 50^o. The internal swirl vanes are arranged in clockwise direction whereas the outer swirler vanes are in anti-clockwise direction, forming a counter-rotating swirl flow motion at the burner outlet. The calculated swirl numbers based on the swirler geometry are S_N ~ 0.78 and 1.04 for the internal and external swirlers (Beer and Chigier, 1972). The relatively high swirl number allows the generation of strong swirl with sufficient intensity to stabilise the flame. A circular quartz tube with the diameter of 100 mm and 150 mm length is used to form the combustor wall at the burner outlet. For the flow delivery system, four mass flow controllers are utilised to supply the gaseous fuel and air to the burner, as shown in Fig. 1. Methane (99.7 % purity, LHV: 50,000 kJ/kg) is used as the source of hydrocarbon fuel. For each annulus, the air and methane supplies are regulated by thermal mass flow controllers (Alicat, ± 1 % accuracy full scale). Premixing of fuel/air occurs at the burner plenum prior to delivery to the burner outlet. The mixtures are ignited at the combustor outlet using a flame torch when both annulus flows have been established.

2.2 Operating conditions

The counter-rotating flames were established at different combination of fuel/air mixtures to enable examination of the flame structures and emission performance. To facilitate descriptions of different operating cases, each established condition is labelled alphanumerically as shown in Table 1. For global flame structure imaging under stratified annulus flow and mixtures, three cases denoted as F1, F2 and F3 were considered. The total air and fuel mass flow rate supplied for all three cases were 7.93 g/s and 0.32 g/s. The total air is split between inner and outer annulus, denoted by the air flow split ratio. The equivalence ratios for the inner and outer annulus mixtures were stratified and maintained constant at ϕ_{in} = 0.71 and ϕ_{out} = 0.68. For emission measurements, two sets of conditions were compared. Case A1-A3 fix the equivalence ratio for inner and outer annulus at ϕ_{in} = 0.67 and ϕ_{out} = 0.83, while varying the air split ratio. For case B1-B3, stratification of the mixtures was inverted, with inner annulus set at ϕ_{in} = 0.83 and outer annulus set at ϕ_{out} = 0.67, with the air flow split ratio varied. Case C1 was established as baseline

reference, where both flames were established at the same equivalence ratio of $\phi_{in,out}$ = 0.75, and swirl air was split between two annuli at the ratio of 50:50.

Table 1: Operating conditions for global flame structure measurement

	Air split ratio[+]		Inner annulus			Outer annulus			
Case	Q_{in} (%)	Q_{out} (%)	$\dot{m}_{air,in}$ (g/s)	$\dot{m}_{fuel,in}$ (g/s)	ϕ_{in}	$\dot{m}_{air,out}$ (g/s)	$\dot{m}_{fuel,out}$ (g/s)	ϕ_{out}	ϕ_{global}
F1	30	70	2.38	0.10	0.71	5.55	0.22	0.68	0.70
F2	50	50	3.96	0.16	0.71	3.96	0.16	0.68	0.70
F3	70	30	5.55	0.23	0.71	2.38	0.09	0.68	0.70
A1	30	70	2.38	0.09	0.67	5.55	0.27	0.83	0.78
A2	50	50	3.96	0.15	0.67	3.96	0.19	0.83	0.75
A3	70	30	5.55	0.22	0.67	2.38	0.11	0.83	0.72
B1	30	70	2.38	0.11	0.83	5.55	0.22	0.67	0.72
B2	50	50	3.96	0.19	0.83	3.96	0.15	0.67	0.75
B3	70	30	5.55	0.27	0.83	2.38	0.09	0.67	0.78
C1*	50	50	3.96	0.17	0.75	3.96	0.17	0.75	0.75

[*] Baseline case; homogenous mixture and even flow rates for both annuli
[+] Total air flow rate is 7.93 g/s and split according to the ratio

3. Results and discussion

3.1 OH* chemiluminescence imaging

The flame structure is investigated using an intensified CCD camera (La Vision) coupled with a UV lens fitted with a bandpass filter centered at 308 ± 10 nm to capture the OH* chemiluminescence emitted from the flames. The intensity of OH* chemiluminescence from the flame can be used as an indicator of heat release, where OH* is produced through oxidation of CH before the final steps in the CH_x reduction chain (Najm et al., 1998). The global flame structures derived from line-of-sight imaging for 3 different cases (F1, F2 and F3) of varied split-air ratio are shown in Figure 2. The inner and outer equivalence ratios are maintained at ϕ_{in} = 0.71 and ϕ_{out} = 0.68 respectively. The flame structures are significantly different depending on air flow split ratio. Overall, two visibly different flame brushes are observed for all established flames. The outlet swirl flame is less intense than the inner swirl flame due to the lean nature of fuel/air mixture. The flame intensity and reaction zone area of the inner swirl flame increases as the flow rate increases. This is attributed to the higher fuel mass flow rate and swirling intensity. The length of the inner swirl flame increases with increased swirling air flow, whereas the outer swirl flame reduces in length with reduced air flow.

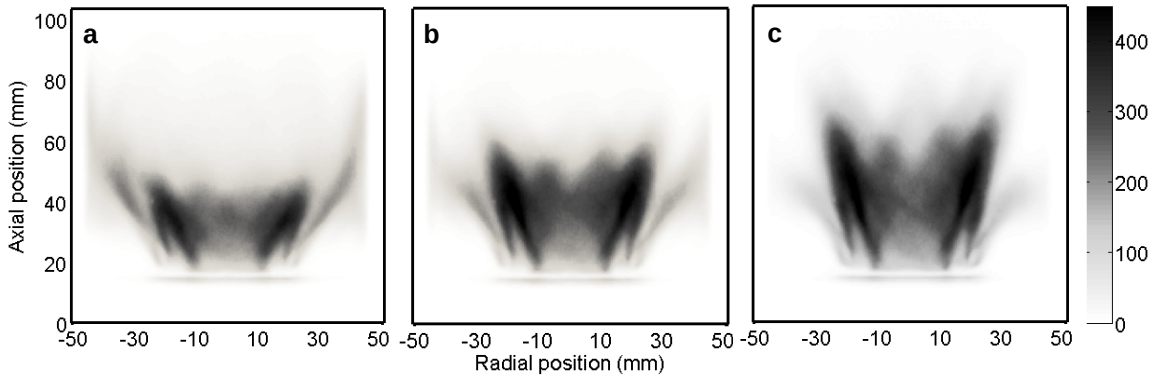

Figure 2: Global OH chemiluminescence images of counter-rotating flame for air flow split ratio of (a) 30:70 (case F1), (b) 50:50 (case F2) and (c) 70:30 (case F3). The inner and outer equivalence ratios are fixed at ϕin = 0.71 and ϕ_{out} = 0.68 respectively*

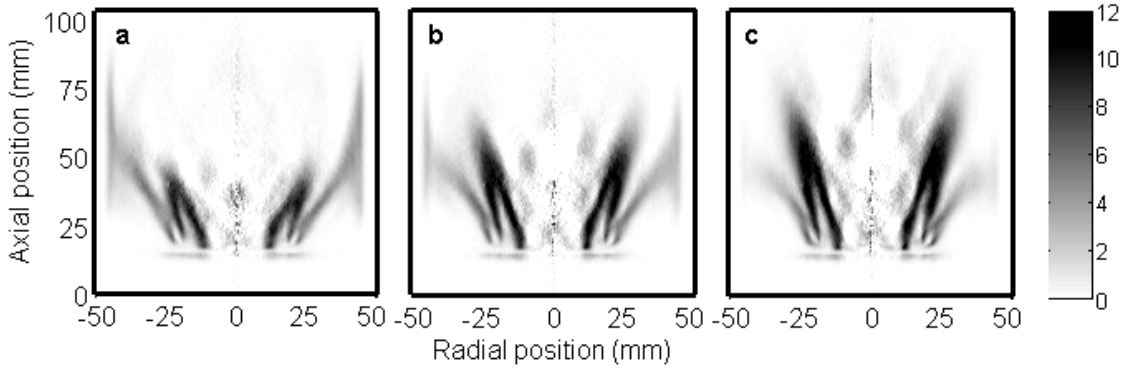

Figure 3: Abel transformed planer OH chemiluminescence images of counter-rotating flame for case (a) F1, (b) F2 and (c) F3*

The line-of-sight global OH* chemiluminescence images are Abel transformed to obtain the planar structure of the flames, as shown in Figure 3(a) to (c). Overall, two different flame fronts from the two annuli are distinguishable, separate by the shear layer between the two flows. The two flame brushes are in close proximity near the burner outlet and flame root, where the shear layer is high as a result of the high relative velocity between the two swirl flows, enhanced further by the counter-rotating swirl motion. The outer annulus flame is pulled towards the wall and the flow diverges to partly form corner recirculation flow while the rest merges with the inner swirl flow to form centre recirculation flow. Inner swirl flame shows higher intensity and larger reaction zone, where the main bulk of heat is release, with highest local temperature.

3.2 Emissions results and discussion

3.2.1 Varied air split ratio, leaner inner/richer outer arrangement

The effect of varied air flow rate between the two annuluses on emissions is investigated. The sampling probe of the gas analyser (Tocsin 320) was placed 10 mm inward from the combustor outlet to sample across half plane of the burner exit. The equivalence ratio for inner and outer annuli are fixed at ϕ_{in} = 0.67 and ϕ_{out} = 0.83. The stratified mixture results in two flames burning at different temperatures. Due to the variation in flow rates, the global equivalence ratio for all three cases are slightly different, as indicated in Table 1. Comparison of the emissions (NO, NO_2 and CO per mass fuel) for these cases is performed based on equal total air and fuel flow by mass, as shown in Figure 4. The emissions for case C1 are shown as baseline reference, where homogenous mixture of $\phi_{in,out}$ = 0.75 was established for respective annulus. In general, all three cases show lower emissions at inner annulus region (r/D = 0-0.2) and increases to higher emissions values at outer annulus region (r/D = 0.3-0.5) due to richer mixture, regardless of the air flow variation between both annuluses. At the lean inner annulus region, case A1 shows lower emissions of NO, NO_2 and CO compared to A2 and A3, which could be due to the lower inner/higher outer swirl flow arrangement that enhances the strength of central recirculation zone. The higher outer flow diverges at the wall to partly form a corner recirculation zone, while the rest of air flow enhances the radial component of the central reverse flow by merging with the central recirculation flow. Mixing of the post-combustion product with the incoming reactants is subsequently improved. The differences in global equivalence ratio due to the varied flow rates affect emissions, as reflected in the rich annulus region. The variation of flow rate does not affect NO and NO_2 emission in general. For CO emission, A3 profile is more level compared to A1 and A2.

3.2.2 Varied air split ratio, richer inner/leaner outer arrangement

In this section, emission performance are measured by fixing the equivalence ratio of inner and outer annulus at ϕ_{in} = 0.83 and ϕ_{out} = 0.67 respectively, while varying the air flow of the two annuluses. Comparison of the emission values against baseline case of C1 is shown in Figure 5. The arrangement of rich inner/lean outer annulus results in higher NO, NO_2 and CO emissions in the inner annulus region (r/D = 0-0.2). These values are significantly higher than the baseline case as expected due to richer flame in the inner annulus. However, emissions at the outer annulus region is either comparable or higher than baseline case, even though the outer annulus flames are much leaner. Case B1 shows NO emission close to C1 at the outer annulus region, but B2 and B3 show emission values higher than baseline case at all spatial locations for NO and NO_2. B2 shows slightly lower CO than baseline at the outer annulus region.

For case B1, emissions of NO, NO_2 and CO at r/D = 0.48 is consistently lower than baseline. This is due to lower equivalence ratio for B1 at the outer annulus coupled with high flow rate near the wall, which suppresses the mixing of emissions from the inner annulus region. In general, the arrangement of rich inner/lean outer annulus is not as favourable as the previous lean inner/rich outer annulus arrangement due to higher emissions, in particular NO and NO_2. CO is also evidently higher for case B1 and B3, although B2 did show some slight reduction at the outer annulus region. No significant advantage with respect to emissions was shown by varying the flow rate of the two annuli.

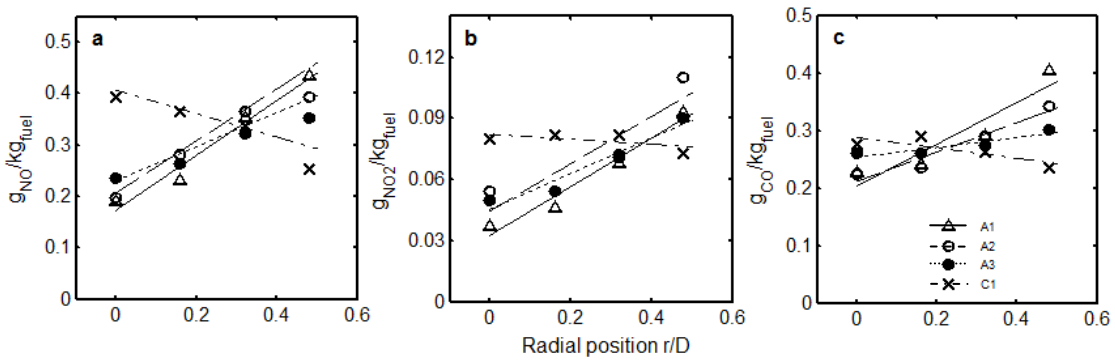

Figure 4: Emission indices of (a) NO, (b) NO_2 and (c) CO for case A1, A2 and A3 (lean inner/rich outer flame) are compared against C1 (homogenous ϕ for both annuli). The air split ratio is varied

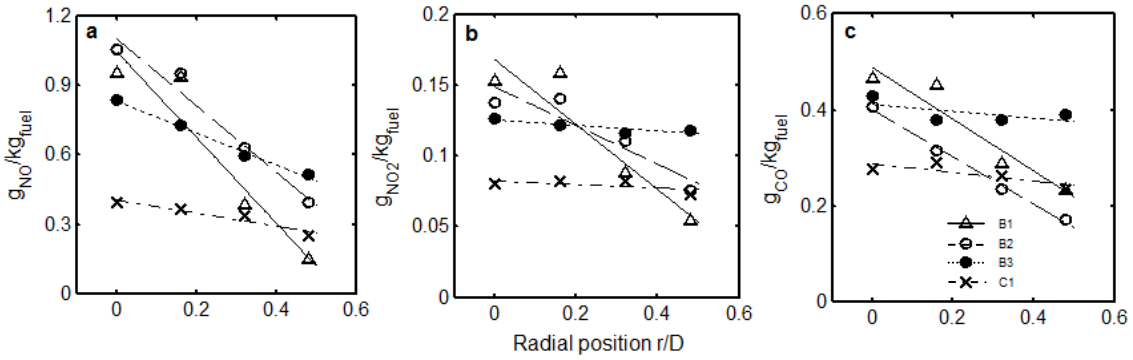

Figure 5: Emission indices of (a) NO, (b) NO_2 and (c) CO for case B1, B2 and B3 (rich inner/lean outer flame) compared against C1 (homogenous ϕ for both annuli). The air split ratio is varied.

3.2.3 Area-velocity weighted emissions

The spatial emission values across the combustor outlet are averaged and area-velocity weighted to obtain final values for comparison. Figure 6 shows the emission indices of NO, NO_2 and CO as a function of air flow split ratio for the arrangements of lean inner/rich outer and rich inner/lean outer annulus. The emissions of homogenous mixture and even air flow for both inner and outer annuli (case C1) are shown as baseline reference. Comparison against C1 shows that the former arrangement (lean inner/rich outer) produces comparable emission performance where NO, NO_2 and CO are only marginally higher than C1. Variation of the air flow split ratio affects the total emissions minimally as the emission is dominated by the equivalence ratios of the two annuluses. The reverse arrangement of rich inner/lean outer shows significantly higher NO and NO_2 compared to C1, whereas for CO, B1 and B3 show higher CO values than C1. The increase of inner annulus flow (correspondingly decrease of outer annulus flow), as in the case of B2 and B3, results in much higher emissions of NO and NO_2 while B3 shows higher CO. For the rich inner/lean outer annulus arrangement, air flow split ratio is a dominant factor that affects emissions.

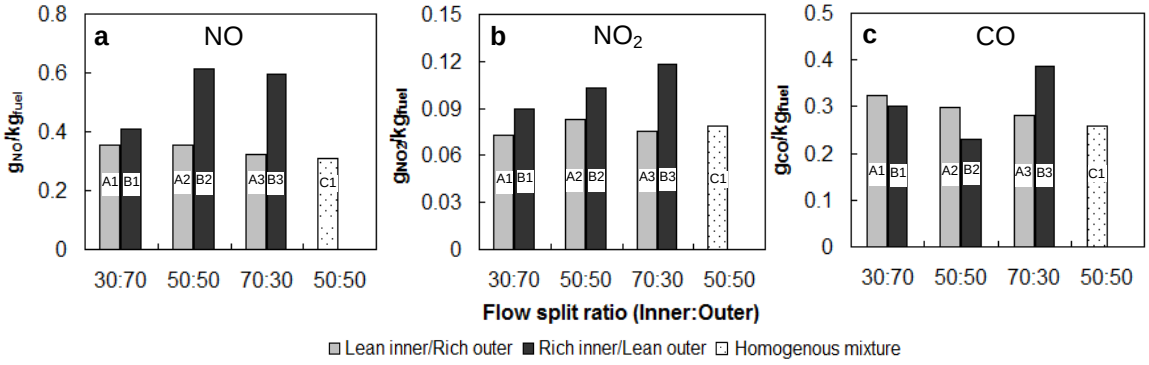

Figure 6: Area-velocity weighted emission indices of (a) NO, (b) NO_2 and (c) CO for the arrangement of lean inner/rich outer (A1,A2 and A3) and rich inner/lean outer (B1, B2 and B3). C1 is baseline case

4. Conclusions

The flame structure and emissions performance of a double annulus counter-rotating swirl flame burner were investigated and characterised. Variation of the mixture equivalence ratios and swirl flow between the inner and outer annulus results in different flame structure. OH* chemiluminescence imaging shows that flame length and reaction zone varies based on the flow and air/fuel mixture stratification. Higher inner annulus flow and richer mixture for inner annulus results in enlarged main reaction zone, increased flame intensity and subsequently higher OH* signals. With respect to emissions, the arrangement of lean inner/rich outer flames results in comparable levels of NO, NO_2 and CO compared to the homogenous mixture and even annulus flows. Variation of flow rate does not affect emission much in the lean inner/rich outer stratification arrangement. The inverse combination, rich inner/lean outer annulus results in higher NO, NO_2 and CO emissions compared to baseline. Higher inner annulus flow results in higher emissions for rich inner/lean outer arrangement.

Acknowledgement

The financial support from the Ministry of Higher Education Malaysia and Universiti Teknologi Malaysia (Research university grant Tier-1 vot no.: 09H79) and Ministry of Science, Technology and Innovation (MOSTI) Malaysia (project number: 03-01-06-KHAS01) is gratefully acknowledged.

References

Ateshkadi A., McDonell V.G., Samuelsen G.S., 1998, Effect of hardware geometry on gas and drop behavior in a radial mixer spray, Symp. (Intl.) Combust., 27, 1985-1992.

Beer J.M., Chigier N.A., 1972, Combustion aerodynamics, Applied Science Publisher, London, UK.

Chong C.T., Hochgreb S., 2014, Spray flame structure of rapeseed biodiesel and Jet-A1 fuel, Fuel 115, 551-558.

Chong C.T., Hochgreb S., 2015, Measurements of Non-reacting and Reacting Flow Fields of a Liquid Swirl Flame Burner. Chinese Journal of Mechanical Engineering, 22, 1-8.

Chong C.T., Hochgreb S., 2015, Spray and combustion characteristics of biodiesel: Non-reacting and reacting, Intl. Biodegradable and Biodegradation, doi:10.1016/j.ibiod.2015.01.012.

Gupta A.K., Lewis M.J., Qi S., 1998, Effect of swirl on combustion characteristics of premixed flames, J. Eng. Gas Turbines Power, 120, 488-494.

Merkle K., Haessler H., Büchner H., Zarzalis N., 2003, Effect of co- and counter-swirl on the isothermal flow- and mixture-field of an airblast atomizer nozzle, Intl. J. Heat Fluid Flow, 24, 529-537.

Najm H.N., Paul P.H., Mueller C.J., Wyckoff P.S., 1998, On the adequacy of certain experimental observables as measurements of flame burning rate, Combust. Flame, 113, 312-332.

Sorrentino G., Sabia P., Joannon M., Cavaliere A., Ragucci R., 2015, Design and development of a lab-scale burner for MILD/flameless combustion, Chemical Engineering Transactions, 43, 883-888

Terasaki T., Hayashi S., 1996, The effects of fuel-air mixing on NOx formation in non-premixed swirl burners, Symp. (Intl.) Combust., 26, 2733-2739.

Vondál J., Hájek J., 2012, Swirling flow prediction in model combustor with axial guide vane swirler, Chemical Engineering Transactions, 29, 1069-1074.